

determines the number of modes into the band pass. On the other hand, the structure of the layout let the identification of the constituent elements of the design in terms of sections which can be theoretically described using transmission matrices representation.

III. CIRCUIT ANALYSIS

Fig. 1(a) shows the proposed MMR-UWB filter layout and Fig. 1(b) the proposed equivalent circuit model based on coupled microstrip transmission lines. The coupled transmission lines are characterized through the even and odd characteristic impedance and electric length (Z_{oe} , θ_e , and Z_{oo} , θ_o respectively). This implies the coexistence of two different modes with different phase velocity and propagating constant corresponding to the different effective relative permittivity.

The even and odd-mode characteristic impedances Z_{oe} and Z_{oo} can be obtained from the expressions:

$$Z_{oe} = \frac{1}{c\sqrt{C_e^a C_e}} \quad (1)$$

$$Z_{oo} = \frac{1}{c\sqrt{C_o^a C_o}} \quad (2)$$

where C_e^a and C_o^a are the even and odd mode capacitances that can be derived directly from the geometrical parameters of the design [9].

The distributed equivalent circuit model showed in Fig.1 (b) can be described by a single ABCD matrix between the input and output ports. Due to the A-A' plane symmetry, the internal structure of this matrix can be described by the Eq.(3)

$$\begin{bmatrix} A & B \\ C & D \end{bmatrix} = M_T M_S M_T M_C M_t M_C M_T M_S M_T \quad (3)$$

Where

$$M_T = \begin{bmatrix} \cos\theta_T & jZ_T \sin\theta_T \\ j\frac{1}{Z_T} \sin\theta_T & \cos\theta_T \end{bmatrix} \text{ and } M_{T'} = \begin{bmatrix} \cos\theta_{T'} & jZ_{T'} \sin\theta_{T'} \\ j\frac{1}{Z_{T'}} \sin\theta_{T'} & \cos\theta_{T'} \end{bmatrix} \quad (4)$$

are the ABCD matrices of the line A and B,

$$M_t = \begin{bmatrix} \cos\theta_t & jZ_t \sin\theta_t \\ j\frac{1}{Z_t} \sin\theta_t & \cos\theta_t \end{bmatrix} \quad (5)$$

is the ABCD matrix associated to the center transmission line D,

$$M_S = \begin{bmatrix} 1 & 0 \\ jZ_S \tan\theta_S & 1 \end{bmatrix} \quad (6)$$

is the ABCD matrix associated to the grounded stub S,

$$M_C = \begin{bmatrix} -Z_{11} & -(Z_{11}^2 - Z_{12}^2) \\ Z_{12} & Z_{12} \\ -1 & -Z_{11} \\ Z_{12} & Z_{12} \end{bmatrix} \quad (7)$$

is the ABCD matrix associated to the coupled lines.

Being the elements of the coupled line:

$$Z_{11} = Z_{22} = \frac{-j}{2} Z_{oe} \cdot \cot(\theta_e) - \frac{j}{2} Z_{oo} \cdot \cot(\theta_o) \quad (8)$$

$$Z_{12} = Z_{21} = \frac{-j}{2} Z_{oe} \cdot \csc(\theta_e) + \frac{j}{2} Z_{oo} \cdot \csc(\theta_o) \quad (9)$$

The physical dimensions showed in Fig.1 (a) correspond to the electrical parameters are $Z_T=44.5 \Omega$, $Z_t=66.6 \Omega$, $Z_s=101.6 \Omega$, $Z_{oe}=145.5 \Omega$, $Z_{oo}=30.5 \Omega$ and 6.5 and 5.8 effective relative dielectric constants for even and odd mode respectively.

Although expressions are complicated [9], the Z_{oe} and Z_{oo} impedances can be analytically evaluated from the substrate thickness (h), the strip width (W) and the separation between coupled lines (S). Fig.2 shows the mapping of these expressions illustrating the fact that for higher S/h relation there is a clear increment of Z_{oo} and a diminution of Z_{oe} . On the other hand, an increment in the W/h ratio implies a reduction of both Z_{oe} and Z_{oo} parameters. According to this map, the extreme values achievable with our fabrication facilities are fixed to $Z_{oe}=145.5 \Omega$ and $Z_{oo}=30.5 \Omega$, corresponding to $W=0.2 \text{ mm}$ and $S=0.03 \text{ mm}$ for a fixed $h=1.27 \text{ mm}$.

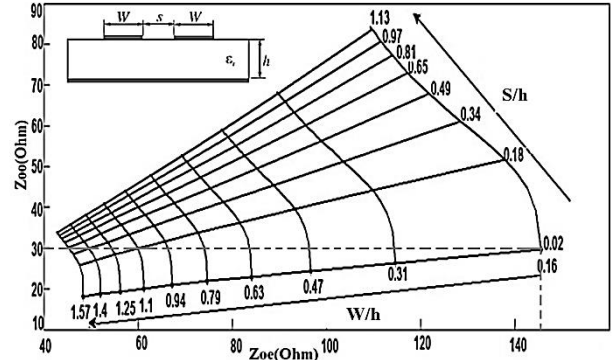


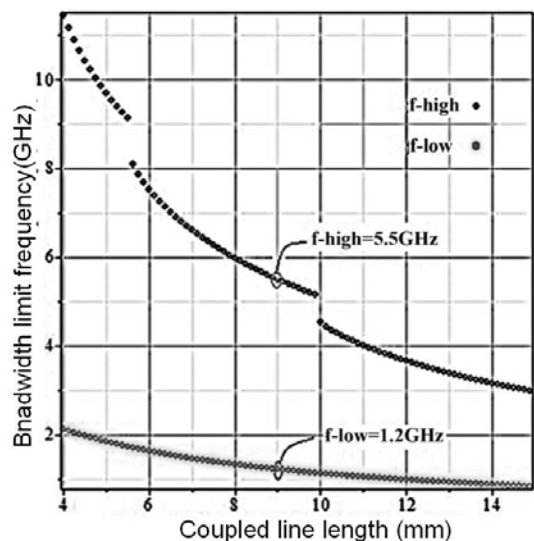
Fig. 2. Even and odd mode (Z_{oe} , Z_{oo} respectively) impedance mapping as function of the S/h and W/h ratios. In all the cases substrate has a fixed value of $h=1.27\text{mm}$ and $\epsilon_r=10.2$.

The resulting ABCD matrix can be used to evaluate the limits of the filter fractional bandwidth (FBW) following the expression.

$$\text{FBW} = \frac{(f_h - f_l)}{f_c} \quad (10)$$

$$f_c = \frac{f_h + f_l}{2} \quad (11)$$

Where f_c denotes the center frequency and higher and lower frequency limits of the bandwidth are represented by f_h and f_l , respectively. It is observed that the center frequency is inversely proportional to the length of coupling line, when the center frequency decreases, the length of coupling line increases. The length of the coupled line of proposed filter is 9 mm long and 0.2 mm wide, the measured high and low frequency are 5.5 GHz, 1.2GHz respectively.



(a)

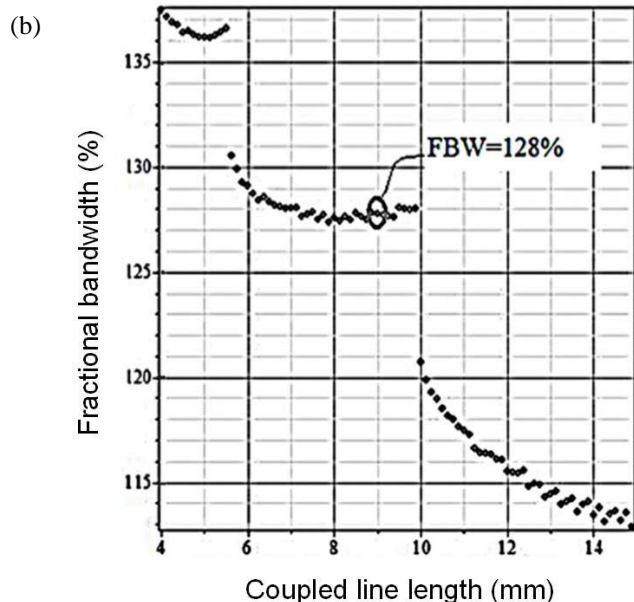


Fig. 3. Show the upper and lower limits of the FBW as a function of the length of the coupled line (D).

Fig.3 shows the upper and lower limits of the MMR-filtering structure (in Fig. 3.a) and the corresponding FBW (in Fig. 3.b) as a function of the length of the coupled line section (see Fig. 1.a). The different number of resonant modes included in the band-pass produces the plateau like behavior observed in Fig. 3.b. For coupled line length below 5 mm there are six resonant modes into the band. In the case of coupled line length between 5 and 10 mm five resonances are included into the MMR design, and four for coupled line length between 10 and 15 mm. As the number of modes into the transmission band increases so does the FBW. However a higher number of resonant modes in the band compromise the rejection band level and the losses in the transmission band frequencies. The proposed design maintains a rejection level below -20 dB with a 128 % FBW at the UWB standard frequencies. The design process can be complex, but due to the equivalent circuit model based on the transmission matrices of the filter sections,

relations between physical parameters and filter performance can be established.

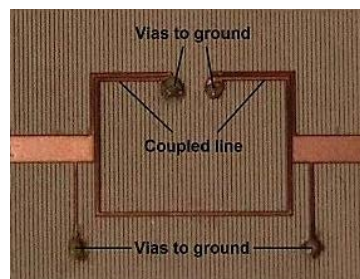
Comparison of fractional bandwidth of this work with other references is given in Table I.

TABLE I
Comparison with other proposed UWB Filters.

Ref.	FBW
[2]	113% @ 2dB
[3]	119% @ 3dB
[5]	114% @ 3dB
[7]	110.6% @ 3dB
This Filter	128% @ 3dB

IV. MEASURED RESULT AND DISCUSSION

As shown in Fig 5, there are five resonant modes generated in the pass band of the MMR filter. Comparing with Fig 3b; it can be seen that, by decreasing lengths of coupled lines, resonant modes are changed. The theory predicts that decreasing coupled line (from 5.5 mm to 5.4 mm), increase band pass filter correlation. The theory was developed and compares well with the measurements parameter of bandwidth. To verify these simulated results, proposed MMR-UWB filter is fabricated and measured by network analyzer. A photograph of the fabricated prototype is shown in Fig. 4.



A. Fig. 4. Photograph of the new compact designed MMR-UWB filter.

The comparison of theoretical, simulation and measurement result shows in Fig .5.

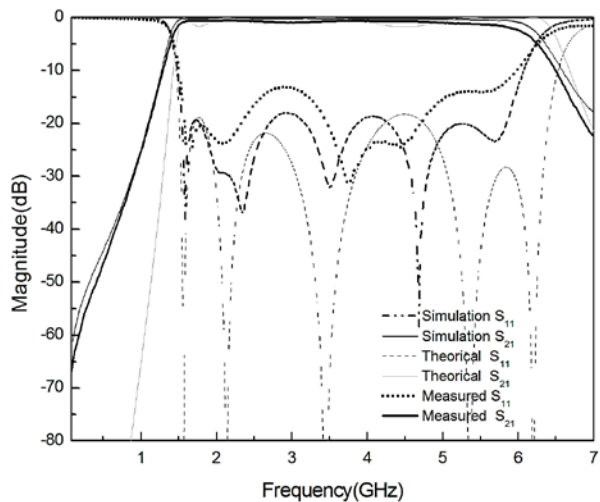


Fig.
5. S-

parameter responses of the EM simulation, theoretical and measurement of MMR-UWB filter.

There is good agreement between the theoretical prediction, simulated and the measured results.

In the measurement, the lower and higher cutoff frequencies of the UWB filter are equal to 1.2 GHz and 5.5 GHz, respectively as can be observed in Fig. 3(a). This indicates that the relevant fractional bandwidth achieves about 128% at the central frequency 2.56 GHz.

V. CONCLUSION

The paper presents a MMR-UWB filter approach with controllable characteristics. Relations between physical parameters and filter performance characteristics such as the central frequency, FBW, or the number of resonant modes into the band-pass have been studied using a distributed transmission matrices model.

REFERENCES

- [1] Z. C. Hao and J. S. Hong, 'Ultra-wideband filters technologies' *IEEE Microw. Mag*, Vol. 11, No. 4, pp. 56-68, 2010
- [2] L. Zhu, S. Sun, and W. Menzel, 'Ultra-wideband (UWB) bandpass filter using multiple-mode resonator', *IEEE Microwave Wireless Compon Lett*, Vol 15, No, 11, pp. 796-798, 2005.
- [3] S. W. Wong and L. Zhu, 'Quadruple-mode UWB bandpass filter with improved out-of-band rejection', *IEEE Microwave Wireless Compon. Lett*, Vol, 19, No, 3, pp. 152-154, 2009.
- [4] L. Han, K. Wu, and X. Zhang, 'Development of packaged ultra-wide band bandpass filters', *IEEE Trans. Microwave Theory Tech*, Vol.58, pp. 220-228, 2010.
- [5] R. Li and L. Zhu, 'Compact UWB bandpass filter using stub-loaded multiple-mode resonator,' *IEEE Microwave Wireless Compon Lett.*, Vol.17, pp. 40-42, 2007.
- [6] K. Song and Y. Fan, 'Compact ultra-wideband bandpass filter using dual-line coupling structure', *IEEE Microwave Wireless Compon. Lett*, 19, pp. 30-32, 2009.
- [7] Z. Shang, X. Guo, B. Cao, V. Wei, X. Zhang, Y. Heng, G. Suo, and X. Song. 'Design of a Superconducting Ultra-

Sideband (UWB) Bandpass Filter with Sharp Rejection Skirts and Miniaturized Size' *IEEE Microwave and Wireless Comp. Lett.*, 23, (2), pp.72-74, 2013.

- [8] H. Ishida and K. Araki, 'Design and analysis of UWB bandpass filter with ring filter', in *IEEE MTT-S Int. Dig.*, 3, pp. 1307-1310, 2004.
- [9] M. J. Lancaster, Jia-Sheng Hong, 'Microstrip Filters for RF/Microwave Applications' John Wiley & Sons, ISBNs: 0-471-38877-7 (Hardback); 0-471-22161-9, 2001.